

# Mistranslation of Membrane Proteins and Two-Component System Activation Trigger Antibiotic-Mediated Cell Death

Michael A. Kohanski,<sup>2,3</sup> Daniel J. Dwyer,<sup>2,4</sup> Jamey Wierzbowski,<sup>2</sup> Guillaume Cottarel,<sup>2</sup> and James J. Collins<sup>1,2,3,\*</sup>

<sup>1</sup>Howard Hughes Medical Institute

<sup>2</sup>Department of Biomedical Engineering, Center for BioDynamics, and Center for Advanced Biotechnology  
Boston University, 44 Cummington Street, Boston, MA 02215, USA

<sup>3</sup>Boston University School of Medicine, 715 Albany Street, Boston, MA 02118, USA

<sup>4</sup>Department of Math and Statistics, 111 Cummington Street, Boston University, Boston, MA 02215, USA

\*Correspondence: jcollins@bu.edu

DOI 10.1016/j.cell.2008.09.038

## SUMMARY

**Aminoglycoside antibiotics, such as gentamicin and kanamycin, directly target the ribosome, yet the mechanisms by which these bactericidal drugs induce cell death are not fully understood. Recently, oxidative stress has been implicated as one of the mechanisms whereby bactericidal antibiotics kill bacteria. Here, we use systems-level approaches and phenotypic analyses to provide insight into the pathway whereby aminoglycosides ultimately trigger hydroxyl radical formation. We show, by disabling systems that facilitate membrane protein traffic, that mistranslation and misfolding of membrane proteins are central to aminoglycoside-induced oxidative stress and cell death. Signaling through the envelope stress-response two-component system is found to be a key player in this process, and the redox-responsive two-component system is shown to have an associated role. Additionally, we show that these two-component systems play a general role in bactericidal antibiotic-mediated oxidative stress and cell death, expanding our understanding of the common mechanism of killing induced by bactericidal antibiotics.**

## INTRODUCTION

Aminoglycosides, such as kanamycin and gentamicin, are a powerful class of bactericidal antibiotics that target the 30S subunit of the ribosome (Davis, 1987). The aminoglycoside family of antibiotics falls into the larger aminocyclitol group of 30S ribosome inhibitors, which also includes the bacteriostatic antibiotic spectinomycin. Protein mistranslation through tRNA mismatching is one of the hallmark phenotypes separating the bactericidal aminoglycosides from the other classes of ribosome inhibitors, including spectinomycin, which are bacteriostatic against *Escherichia coli* (*E. coli*) (Davis, 1987; Weisblum and Davies, 1968). Other phenotypes associated with aminoglycoside

uptake and lethality include changes in membrane potential and permeability (Bryan and Kwan, 1983; Taber et al., 1987).

The lethal mode of action of aminoglycosides is thought to be due to either insertion of misread proteins into the inner membrane of *E. coli* (Bryan and Kwan, 1983; Davis et al., 1986) or irreversible uptake of aminoglycosides leading to complete inhibition of ribosome function (Davis, 1987); however, it is still unclear how this latter proposed mechanism contributes to aminoglycoside-mediated killing (Vakulenko and Mobashery, 2003). It has also been suggested that the mechanism of aminoglycoside-induced lethality is a function of more than ribosome inhibition and may be due to inhibition of multiple cellular targets (Hancock, 1981). In addition, there is a correlation between abnormal protein synthesis, such as mistranslation, and protein carbonylation, a form of oxidative stress (Dukan et al., 2000).

We have proposed that bactericidal antibiotics, including aminoglycosides, induce reactive oxygen species formation, which contributes to drug-mediated cell death (Kohanski et al., 2007). In this proposed model, bactericidal antibiotics perturb metabolism and respiration, leading to increased superoxide production and release or exposure of ferrous iron, which interacts with endogenous hydrogen peroxide to form lethal hydroxyl radicals (Dwyer et al., 2007; Kohanski et al., 2007). The sequence of events following the initial drug-target interaction that generate an intracellular environment promoting hydroxyl radical formation remains unknown for the different classes of bactericidal antibiotics.

In this study, we have elucidated the biological events following aminoglycoside interaction with the ribosome that lead to reactive oxygen species formation and contribute to cell death. Through systems-level approaches together with phenotypic and biochemical studies, we show that the protein translocation machinery and the Cpx envelope stress-response two-component system play important roles in oxidative stress-related cell death induced by aminoglycosides. We present evidence that the redox-responsive Arc two-component system is involved in this event, possibly via crosstalk between the Cpx and Arc two-component systems. Our results indicate that aminoglycoside-induced free radical formation is triggered by two-component stress-response system sensing of misfolded proteins in

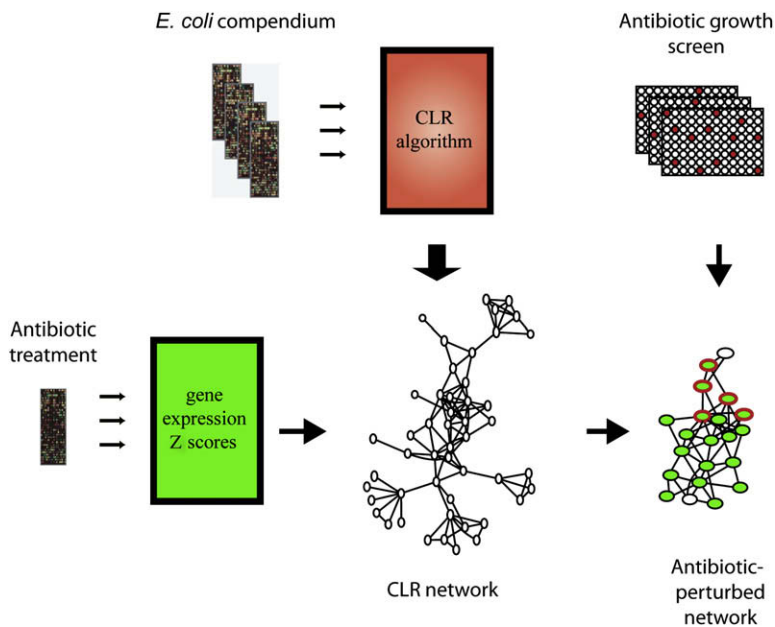


### Figure 1. Identification of Pathways Related to Aminoglycoside Lethality

Significantly changing genes from a comparison of treatment with a lethal aminoglycoside versus the bacteriostatic ribosome inhibitor spectinomycin, were filtered through an *E. coli* gene connectivity map generated with the context likelihood of relatedness algorithm (Faith et al., 2007); the resultant gene networks were analyzed for functional enrichment. The strains exhibiting decreased growth or increased growth found from a high-throughput screen of an *E. coli* single-gene deletion library treated with gentamicin were overlaid on these networks.

to extract groups of functionally related genes (Figure 1) and gave us greater ability to focus on specific pathways related to aminoglycoside mode of action. We also examined previously collected expression profiles (Kohanski et al., 2007) after treatment with the aminoglycoside kanamycin and compared these to expression profiles after treatment with spectinomycin. Among the gene networks identified, there were six in common between gentamicin and kanamycin treatment (Figure 2 and Figure S1), and these networks were analyzed for pathway and transcription factor enrichment (see the Experimental Procedures) (Table S2).

In addition to our gene expression analysis, we also utilized a high-throughput screen of an *E. coli* single-gene deletion library (Baba et al., 2006) treated with gentamicin (Table S3; see the Experimental Procedures) to identify potential gene targets with increased sensitivity to gentamicin (Table S4). The gene networks (Figure 2 and Figure S1) were further enriched with the growth data derived from the high-throughput screen of the *E. coli* single-gene deletion library.

Among the networks related to aminoglycoside lethality, one (Figure 2A) showed enrichment ( $p < 10^{-11}$ ) for ArcA-regulated elements of the electron transport chain, the tricarboxylic acid (TCA) cycle, and respiration. ArcA is part of the Arc two-component system. In general, two-component systems, which take part in important bacterial processes such as the cell cycle and virulence (Hoch, 2000), consist of a sensor protein and a cognate transcription factor; the activity of the transcription factor is modulated by the sensor protein. The Arc two-component system consists of a quinone-sensitive sensor kinase, ArcB, which responds to the redox state of the cellular quinone pool by regulating the phosphorylation state of the transcription factor, ArcA (Georgellis et al., 2001; Malpica et al., 2004). In addition, ArcA activation leads to changes in expression of many genes involved in respiration and metabolism (Liu and De Wulf, 2004).

We have previously shown that deletion of some of the TCA cycle genes in this metabolism-related network (Figure 2A) attenuate bactericidal antibiotic-mediated cell death (Kohanski et al., 2007). Many of these single-deletion knockouts exhibit increased growth in the presence of gentamicin (Figure 2A). In addition, we found, via qPCR, that the vast majority of ArcA-regulated TCA cycle genes tested exhibited a significant spike in gene expression within the first 30 min after exposure to gentamicin (Figure S2A). Importantly, the changes in expression

the membrane and periplasmic space, which shifts the cell into a state that stimulates and fuels oxygen radical generation and ultimately results in cell death. Importantly, we also demonstrate that the envelope stress-response and redox-responsive two-component systems are broadly involved in bactericidal antibiotic-mediated oxidative stress and cell death, providing additional insight into the common mechanism of killing induced by bactericidal antibiotics.

## RESULTS

### Gene Expression Analysis of Pathways Related to Aminoglycoside Lethality

We utilized gene expression microarrays and statistical analyses (see the Experimental Procedures) to compare gene expression profiles of wild-type (MG1655) *E. coli* treated with the aminoglycoside gentamicin to expression profiles after treatment with the bacteriostatic ribosome inhibitor spectinomycin (Table S1 available online). Statistically significant changes in expression (z score) were determined on a gene-by-gene basis by comparison of mean expression levels to a large (~525) compendium of *E. coli* microarray data collected under a wide variety of conditions (see the Experimental Procedures). We then examined the relative changes in z score between bactericidal- and bacteriostatic-treated samples. This allowed us to separate gene expression changes related to aminoglycoside lethality and hydroxyl radical formation from aminoglycoside effects on cell growth.

To identify networks related to aminoglycoside lethality, we filtered the set of significantly changing genes through an *E. coli* gene connectivity map generated using the context likelihood of relatedness (CLR) algorithm (Faith et al., 2007). Among the CLR-predicted connections, only those between genes that were significantly perturbed (on the basis of z score changes) and connections where one nonperturbed gene connected two significantly perturbed genes were maintained. This allowed us

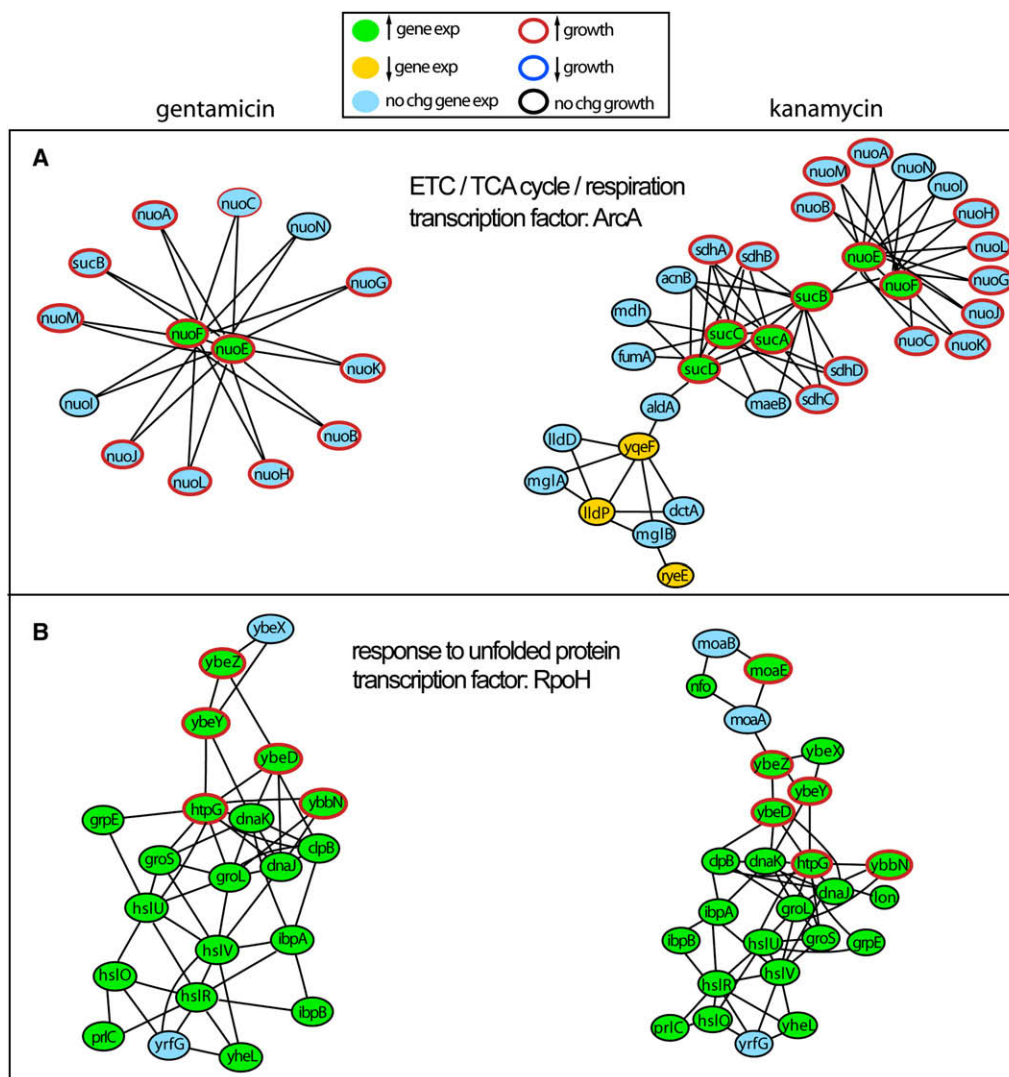


**Figure 2. CLR-Based Networks of Genes Whose Expression Changed Significantly Because of Gentamicin or Kanamycin Treatment**

In this figure, upregulated gene expression is shown in green, downregulated gene expression is shown in yellow, and nonperturbed gene expression is shown in light blue. Overlaid on these networks are the outliers from a screen of the single-deletion knockout (KO) library grown in the presence of 5  $\mu\text{g}/\text{ml}$  gentamicin (increased growth of KO, red rim; decreased growth of KO, blue rim; no change in growth of KO, black rim). We note that no single knockouts of genes in these networks show decreased growth in the presence of gentamicin.

(A) Network of genes showing pathway enrichment for the electron transport chain (ETC), tricarboxylic acid (TCA) cycle, and respiration ( $p < 10^{-11}$ ), and transcription factor enrichment for metabolic regulators including ArcA ( $p = 1.8 \times 10^{-12}$ ).

(B) Network of genes showing pathway enrichment for the response to misfolded proteins ( $p = 1 \times 10^{-17}$ ) and the heat shock sigma factor,  $\sigma^H$  (RpoH;  $p = 1.2 \times 10^{-11}$ ).

among the genes in this ArcA-regulated metabolic gene network are consistent with the previously described roles of metabolism and respiration in bactericidal antibiotic-induced hydroxyl radical formation and cell death (Kohanski et al., 2007).

Our systems-level analysis also highlighted a network related to protein mistranslation, which is one of the phenotypes specifically associated with the aminoglycoside family of ribosome inhibitors (Davis, 1987; Weisblum and Davies, 1968). This network (Figure 2B) showed significant enrichment for the response to misfolded proteins ( $p = 1 \times 10^{-17}$ ) by proteases regulated by the heat shock sigma factor,  $\sigma^H$  (RpoH). These proteases were significantly upregulated in response to bactericidal aminoglyco-

side treatment (Figure 2B). This suggests that aminoglycoside-driven protein mistranslation and subsequent misfolding may be a necessary component required to drive lethal hydroxyl radical formation.

In addition to a metabolic network and a protease network, the gentamicin and kanamycin treatments brought to light a large network of transport protein-related genes ( $p < 0.05$ ) (Table S2). This network contains genes associated with electrochemical gradient-driven transport across the cell membrane, including genes involved in sugar and phosphate transport (Table S2). This transport-related network may reflect aminoglycoside-specific protein mistranslation and subsequent misfolding of

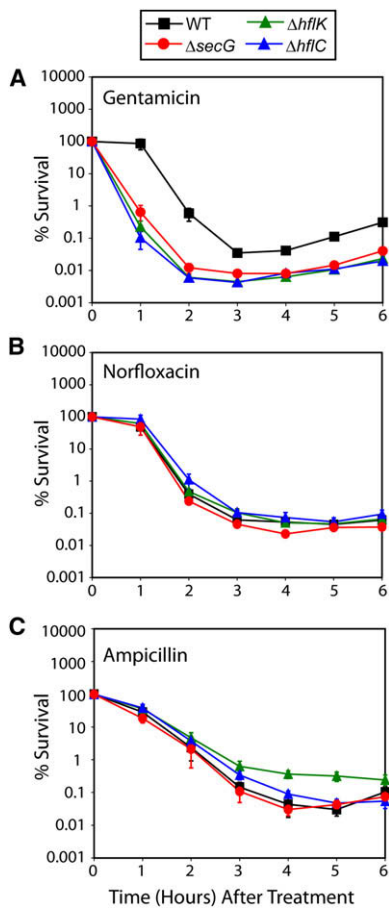


**Figure 3. Disrupting Membrane Regulatory Systems Enhances Aminoglycoside Lethality**

Percent survival of wild-type *E. coli* (black squares),  $\Delta secG$  (red circles),  $\Delta hflK$  (green triangles), and  $\Delta hflC$  (blue triangles) after treatment with 5  $\mu$ g/ml gentamicin (A), 100 ng/ml norfloxacin (B), or 3  $\mu$ g/ml ampicillin (C). Mean  $\pm$  SEM are shown for all figures.

membrane proteins, which would have a cumulative effect on the electrochemical potential and integrity of the membrane.

### Aminoglycoside-Induced Mistranslation of Membrane Proteins Induces Hydroxyl Radical Formation and Cell Death

On the basis of our expression analysis, we focused our attention on genes and pathways associated with fidelity of membrane proteins to determine whether these systems are functionally linked to aminoglycoside-induced oxidative stress and lethality. An analysis of our high-throughput growth screen (Table S3) revealed 11 single-gene knockouts exhibiting significant decreases in growth after gentamicin treatment (Table S4). Among these 11 genes, three of the gene products, HflK, HflC, and SecG, are involved in the regulation of membrane proteins, and two of the genes, *hflK* and *hflC*, show a significant increase in expression after aminoglycoside treatment (Tables S5 and S6).

In *E. coli*, protein trafficking through the inner membrane occurs via multiple pathways, including the Sec and signal recog-

nition particle (SRP) translocation systems. The Sec and SRP pathways utilize a chaperone-based system to shuttle immature proteins to the SecYEG translocase protein complex for transport across the inner membrane (Danese and Silhavy, 1998b; Economou, 1999; Luirink and Sinning, 2004; Mori and Ito, 2001; Wickner and Schekman, 2005). Immature proteins are targeted to the Sec translocase (SecY, SecE, and SecG) by chaperones (SecB or the SRP system) and processed through the SecYEG translocase by the translocation ATPase SecA (Economou, 1999; Hartl et al., 1990; Luirink and Sinning, 2004; Mori and Ito, 2001). SecG works in conjunction with SecA to promote efficient protein translocation (Matsumoto et al., 1998). HflK and HflC together negatively regulate FtsH (Kihara et al., 1996, 1997; Saikawa et al., 2004), and loss of HflK or HflC should diminish the ability of FtsH to degrade membrane-associated proteins, including SecY and  $\sigma^H$  (Akiyama et al., 1996; Gottesman, 1996; Kihara et al., 1999).

To determine whether translocation of mistranslated proteins across or into the inner membrane specifically enhances killing by aminoglycosides, we initially focused on three single-gene knockouts— $\Delta secG$ ,  $\Delta hflK$ , and  $\Delta hflC$ . We treated them with the mistranslation-inducing aminoglycoside gentamicin, the DNA gyrase inhibitor norfloxacin, the cell wall synthesis inhibitor ampicillin, and the bacteriostatic, mistranslation-free aminocyclitol, spectinomycin (see the Supplemental Data for results with spectinomycin), respectively. Additionally, we examined survival at both a clinically relevant level of gentamicin (5  $\mu$ g/ml) and at a substantially higher concentration (15  $\mu$ g/ml) (Zaske et al., 1982).  $\Delta secG$ ,  $\Delta hflK$ , and  $\Delta hflC$  treated with 5  $\mu$ g/ml gentamicin each exhibited a significant increase in both the rate of killing and overall cell death relative to wild-type *E. coli* treated with gentamicin (Figure 3A). In contrast, when these single-deletion strains were treated with 100 ng/ml norfloxacin (Figure 3B) or 3  $\mu$ g/ml ampicillin (Figure 3C), cell killing was quite similar to that seen with the wild-type. This demonstrates that the increase in cell death observed in  $\Delta secG$ ,  $\Delta hflK$ , and  $\Delta hflC$  is specific to the lethal mechanism of action of aminoglycosides. Treatment of  $\Delta secG$ ,  $\Delta hflK$ , or  $\Delta hflC$  with a higher concentration of gentamicin (15  $\mu$ g/ml) significantly reduced the difference in viability between these strains and the wild-type (Figure S4). It is worth noting that the remainder of the single-gene deletions identified in Table S4 did not display increased efficacy of killing by gentamicin (Figures S5 and S6; see the Supplemental Data for further discussion).

SecG has a known role in promoting efficient protein translocation (Matsumoto et al., 1998), whereas the HflKC complex regulates FtsH, thereby affecting the degradation of membrane-associated proteins (Akiyama et al., 1996; Gottesman, 1996; Kihara et al., 1999). Changes to these SecG- or HflKC-regulated functions affect movement of mistranslated proteins across the membrane, which may account for the observed increase in cell death (Figure 3A) after aminoglycoside treatment of  $\Delta hflK$ ,  $\Delta hflC$ , or  $\Delta secG$ ; see the Supplemental Data for further discussion.

We examined how these single-gene deletions affect hydroxyl radical formation and membrane depolarization to determine whether there is a relationship between these phenomena and an increase in translocation of mistranslated proteins across the inner membrane. Both radical formation (Kohanski et al., 2007) and changes in membrane potential (Bryan and Kwan,

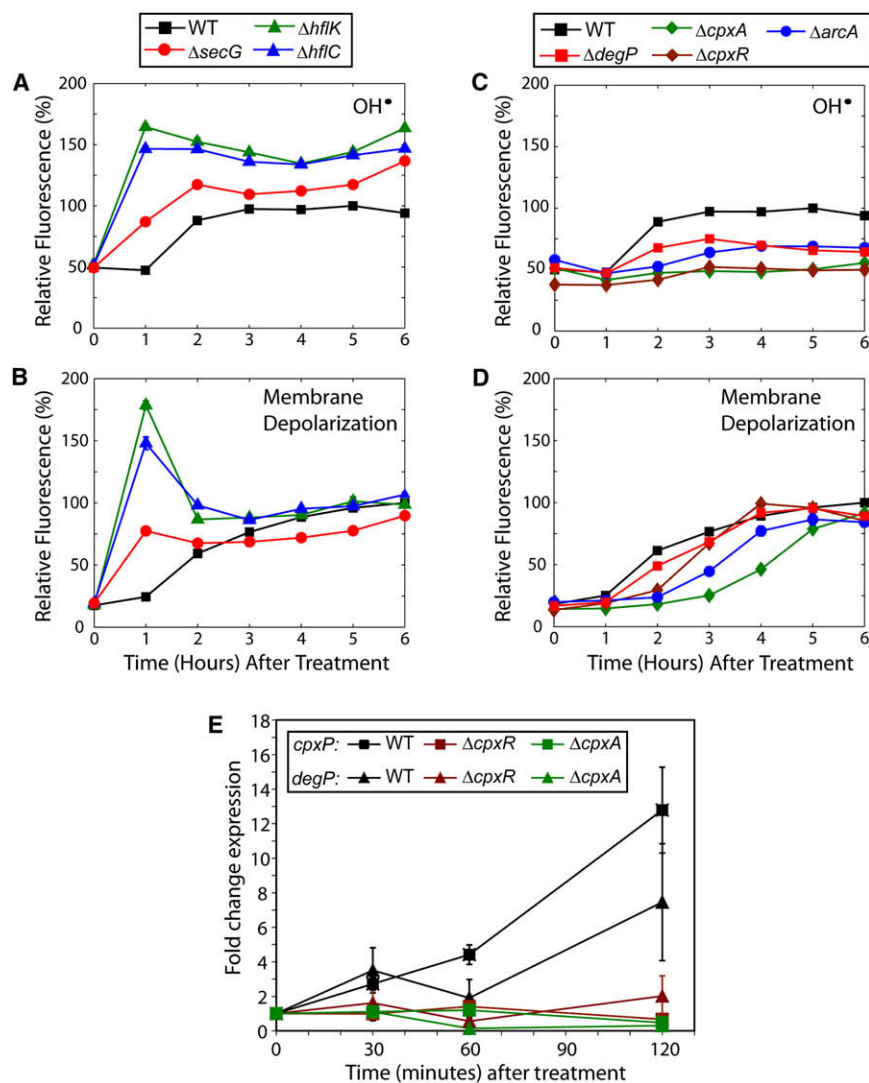


**Figure 4. Disruption of Membrane Regulatory Systems and the Envelope Stress Response Enhances Aminoglycoside-Induced Hydroxyl Radical Formation and Membrane Depolarization**

(A–D) Fluorescence for each strain relative to the maximum fluorescence achieved in the wild-type background with the hydroxyl radical-detecting dye HPF (A and C) or the membrane depolarization dye DIBAC<sub>4</sub>(3) (B and D). Hydroxyl radical formation (A) and membrane depolarization (B) of wild-type *E. coli* (black squares),  $\Delta secG$  (red circles),  $\Delta hflK$  (green triangles) and  $\Delta hflC$  (blue triangles) after treatment with 5  $\mu$ g/ml gentamicin are shown. Hydroxyl radical formation (C) and membrane depolarization (D) of wild-type *E. coli* (black squares),  $\Delta degP$  (red diamonds),  $\Delta cpxA$  (green diamonds),  $\Delta cpxR$  (red diamonds), and  $\Delta arcA$  (blue circles) after treatment with 5  $\mu$ g/ml gentamicin are shown.

(E) Fold-change gene expression relative to baseline ( $t = 0$  min) of the envelope stress-response genes, *cpxP* (squares), and *degP* (triangles), for wild-type *E. coli* (black),  $\Delta cpxR$  (brown), and  $\Delta cpxA$  (green) after treatment with 5  $\mu$ g/ml gentamicin.

1983; Taber et al., 1987) have been associated with aminoglycoside-mediated lethality. Consistent with the increase in killing efficacy and trafficking of mistranslated membrane proteins after aminoglycoside treatment, we found that there was significantly more hydroxyl radical formation [measured with the dye 3'-(p-hydroxyphenyl) fluorescein (HPF) (Setsukinai et al., 2003)] in  $\Delta hflK$ ,  $\Delta hflC$ , or  $\Delta secG$  than in the wild-type (Figure 4A). In addition, hydroxyl radical formation occurred by 1 hr after addition of gentamicin in these three mutants, compared to 2 hr in the wild-type (Figure 4A).

If aminoglycoside-induced hydroxyl radical formation is in fact related to disruption of the electrochemical gradient because of improper trafficking of corrupt membrane proteins, the changes in membrane potential associated with aminoglycoside treatment should reflect changes in hydroxyl radical formation. We observed a gradual increase in membrane depolarization [measured with the dye DIBAC<sub>4</sub>(3), which differs from fluorescent intercalating dyes in that it can diffuse across depolarized yet intact cell membranes (Jepras et al., 1997)] in wild-type *E. coli* by 2 hr (Figure 4B), which was consistent with the

onset of cell death (Figure 3A) and hydroxyl radical formation (Figure 4A).  $\Delta hflK$ ,  $\Delta hflC$ , and  $\Delta secG$  all exhibited a significant increase in membrane depolarization by 1 hr (Figure 4B), which correlates with the significant increase in hydroxyl radical formation beyond wild-type levels (Figure 4A). The spikes in depolarization observed at 1 hr for  $\Delta hflK$ ,  $\Delta hflC$ , and  $\Delta secG$  (Figure 4B) suggest a more complex role for membrane potential as related to membrane

#### Involvement of the Envelope Stress-Response and Redox-Responsive Two-Component Systems in Drug-Mediated Cell Death

Our results with  $\Delta secG$ ,  $\Delta hflK$ , and  $\Delta hflC$  point toward a relationship among aminoglycoside-induced changes in membrane protein translocation, membrane depolarization, and hydroxyl radical formation resulting in rapid cell death. Early changes in membrane depolarization may reflect changes in the redox state of the cell that are regulated, in part, by changes in expression of ArcA-regulated metabolic genes (Figure S2). In addition, membrane depolarization may also reflect changes in membrane properties because of aminoglycoside-induced trafficking of mistranslated proteins across the inner membrane.

Once proteins are translocated across the membrane, several overlapping cell envelope maintenance and stress-response systems (including the Cpx envelope stress-response two-component system) are responsible for peptide quality control

functions including, for example, regulation of protein abundance, signal sequence cleavage, and degradation of misfolded/mistargeted species (Duguay and Silhavy, 2004). Disruption of envelope proteins should activate the Cpx envelope stress-response two-component system. The Cpx two-component system monitors the fidelity of proteins trafficked across the inner membrane via the membrane-bound CpxA sensor, which in turn phosphorylates the transcription factor CpxR (Ruiz and Silhavy, 2005). CpxR works in conjunction with  $\sigma^E$  (RpoE) to regulate the expression of envelope stress-response genes, such as the periplasmic protease DegP (Danese et al., 1995; Pogliano et al., 1997; Ruiz and Silhavy, 2005; Strauch et al., 1989).

Interestingly, there is also evidence for crosstalk between the Cpx envelope stress-response and Arc redox responsive two-component systems, pointing toward a link between envelope stress and fluctuations in metabolism. In fact, CpxA was the original two-component sensor linked with ArcA-mediated changes on the basis of phenotypes associated with F pilus formation (Iuchi et al., 1989; Ronson et al., 1987). Using qPCR, we examined gene expression changes over time for ArcA-regulated TCA cycle genes (Figure S10) along with genes from the NADH dehydrogenase I, *nuo* operon (Figure S11), in  $\Delta arcA$ ,  $\Delta cpxA$ , and  $\Delta cpxR$  after gentamicin treatment. The results (see the Supplemental Data for more details) show uncompensated activation of ArcA-regulated genes for  $\Delta arcA$ ,  $\Delta cpxA$ , and  $\Delta cpxR$  relative to wild-type after gentamicin treatment (Figures S2, S10, and S11). Based on our previous work (Dwyer et al., 2007; Kohanski et al., 2007), fluctuations in metabolism should promote an environment conducive toward oxidative damage. Accordingly, we observed, by qPCR, increased expression of oxidative stress-response genes, including *soxS* and OxyR-regulated genes (Figure S8; see the Supplemental Data for further discussion).

We also confirmed by qPCR that aminoglycosides induced significant, sustained changes in expression of the CpxR-regulated envelope stress-response genes *degP* and *cpxP* within the first 30 min after treatment with gentamicin (Figure 4E). We confirmed that these changes require a functional Cpx two-component system (Figure 4E). Our phenotypic results with  $\Delta secG$ ,  $\Delta hflK$ , and  $\Delta hflC$  (Figures 3 and 4), coupled with these qPCR results (Figure 4E), suggest that modulation of Cpx-controlled pathways may be an important regulator of cell death triggered by aminoglycoside-induced protein mistranslation.

To determine whether aminoglycoside-induced stimulation of the Cpx envelope stress-response system is involved in membrane depolarization and induction of an oxidative response, we examined hydroxyl radical formation and membrane depolarization in  $\Delta cpxA$  and  $\Delta cpxR$ . We chose to examine a *degP* knockout as well because DegP, as a periplasmic protease, is a key downstream element of the envelope stress response and because we found that *degP* expression increased after treatment with gentamicin (Figure 4E). We also examined  $\Delta arcA$  because of the potential for crosstalk with CpxA and the ability of ArcA, as a major transcription factor, to affect numerous redox-based pathways.

Hydroxyl radical formation, measured with the dye HPF, was completely attenuated in  $\Delta cpxA$  and  $\Delta cpxR$  treated with gentamicin and significantly reduced in  $\Delta degP$  and  $\Delta arcA$  treated with gentamicin (Figure 4C). We also observed a significant delay in membrane depolarization relative to the wild-type after gentami-

cin treatment of  $\Delta cpxA$ ,  $\Delta cpxR$ ,  $\Delta degP$ , and  $\Delta arcA$  (Figure 4D). These data show that aminoglycoside-induced radical formation and membrane depolarization require an intact Cpx signaling pathway as well as a functional ArcA system.

We next examined survival in  $\Delta cpxA$ ,  $\Delta cpxR$ ,  $\Delta degP$ , and  $\Delta arcA$  treated with gentamicin to determine whether the changes in radical formation and membrane potential correlated with cell survival.  $\Delta cpxA$ ,  $\Delta cpxR$ , and  $\Delta arcA$  exhibited significant increases in survival relative to wild-type *E. coli* during the initial 4 hr after treatment with 5  $\mu\text{g/ml}$  gentamicin (Figure 5A). Colony-forming capability in  $\Delta cpxA$  and  $\Delta arcA$  actually increased for the first 3 hr after addition of gentamicin, and significant killing was not observed in these strains until 5 hr into the treatment (Figure 5A).  $\Delta degP$  exhibited a significant delay in the rate of killing relative to the wild-type after gentamicin treatment (Figure 5A). These results are consistent with the observed decreases in radical formation and membrane depolarization for the respective strains (Figures 4C and 4D) and further point toward a relationship between membrane protein mistranslation, the envelope stress response, radical formation, and cell death.

Although treatment of  $\Delta cpxA$ ,  $\Delta cpxR$ ,  $\Delta degP$ , and  $\Delta arcA$  with gentamicin showed significant delays in killing, cell death does eventually occur in these strains (Figure 5A). This killing is independent of radical formation (Figure 4C) but does correlate with the gradual increases in membrane depolarization (Figure 4D). These results suggest that aminoglycosides utilize multiple means of killing to achieve efficient cell death in *E. coli*.

CpxR and ArcA are key transcription factors with regulatory effects across a large number of genes and pathways. Although the association between increased cell death and mistranslated membrane proteins appears to be specific to aminoglycosides (Figure 3), the cooperativity existent between translocation pathways, envelope stress sensors and response systems, and the redox state of the cell is critical for preservation of membrane integrity and cellular viability and may have a broader role in drug-mediated cell death. Given the overall importance of membrane integrity to cellular viability, we also examined survival of  $\Delta cpxA$ ,  $\Delta cpxR$ ,  $\Delta degP$ , and  $\Delta arcA$ , respectively, after treatment with 100 ng/ml norfloxacin or 3  $\mu\text{g/ml}$  ampicillin (Figures 5B and 5C). (We also treated these strains with higher concentrations of bactericidal antibiotics to determine the effect of drug concentration on survival in these knockout strains; see the Supplemental Data for further details; Figure S9.)

$\Delta cpxA$  and  $\Delta cpxR$  each exhibited increased survival after treatment with norfloxacin or ampicillin (Figure 5B).  $\Delta arcA$  exhibited increased survival after treatment with norfloxacin (Figure 5B) and a delay in killing after treatment with ampicillin (Figure 5C). Interestingly,  $\Delta cpxA$  has a clear increase in survival after 4 hr of treatment with ampicillin. We also note that wild-type *E. coli* exhibited a clear increase in survival after 3 to 4 hr of treatment with gentamicin or ampicillin but not norfloxacin (Figure 5). This effect appears to be concentration dependent (see the Supplemental Data for further discussion; Figure S9). A delay in killing was observed with  $\Delta degP$  after treatment with ampicillin (Figure 5B), a drug that directly targets the cell wall.  $\Delta degP$  displayed wild-type levels of killing after treatment with norfloxacin (Figure 5C), a drug that does not directly affect the membrane. These results suggest that the envelope stress-response and

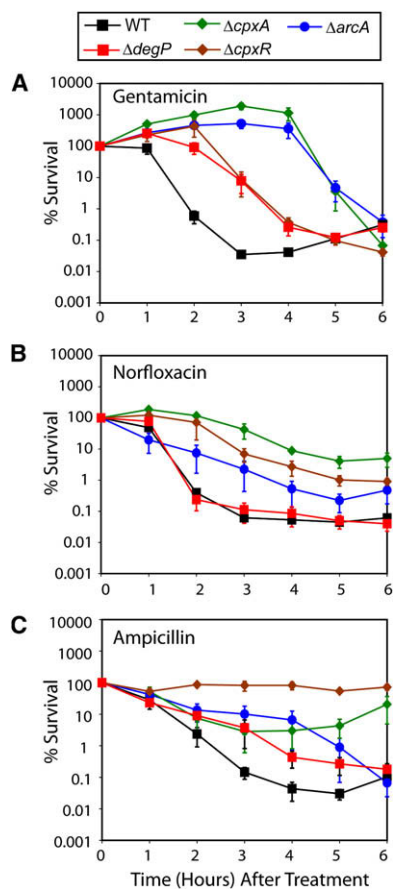


**Figure 5. The Envelope Stress-Response and Redox-Responsive Two-Component Systems Are Involved in Bactericidal Drug-Mediated Lethality**

Percent survival of wild-type *E. coli* (black squares),  $\Delta degP$  (red diamonds),  $\Delta cpxA$  (green diamonds),  $\Delta cpxR$  (red diamonds), and  $\Delta arcA$  (blue circles) after treatment with 5  $\mu$ g/ml gentamicin (A), 100 ng/ml norfloxacin (B), or 3 mg/ml ampicillin (C).

redox-responsive two-component systems have broad roles in bactericidal antibiotic-mediated cell death.

### The HflKC and SecG Systems Trigger Aminoglycoside Killing through Two-Component System Activation

Loss of function of SecG or the HflKC complex in their respective knockout strains led to an abrupt increase in membrane depolarization, hydroxyl radical formation, and cell death (Figures 3 and 4). This is likely due to changes in the accumulation and rate of trafficking of mistranslated membrane proteins (Figure S7), which should, in turn, affect signaling via CpxA. To confirm that activation of the Cpx and Arc two-component systems triggers membrane depolarization and hydroxyl radical formation after aminoglycoside treatment in  $\Delta secG$  and  $\Delta hflK$ , we examined survival, hydroxyl radical formation, and membrane depolarization after deletion of *cpxA* or *arcA* in  $\Delta secG$  and  $\Delta hflK$ , respectively. As expected, the increases in killing, hydroxyl radical formation, and membrane depolarization observed in  $\Delta secG$  and  $\Delta hflK$  were significantly reduced when either *cpxA* or *arcA* was

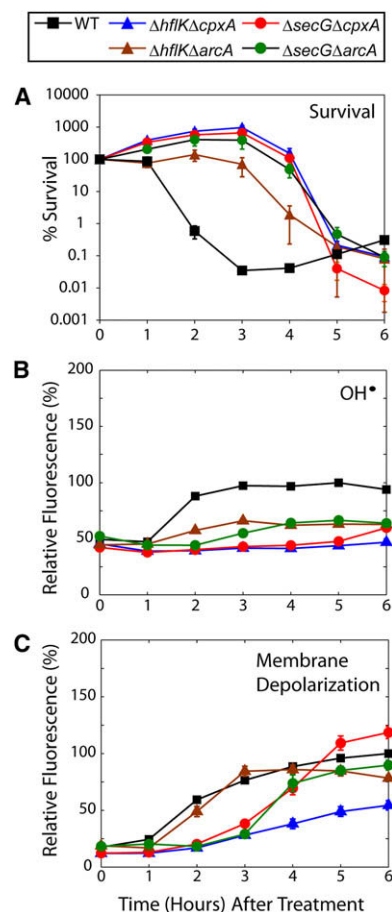


**Figure 6. Envelope Stress-Response and Redox-Responsive Two-Component Systems Trigger Hydroxyl Radical Formation Because of Mistranslation of Membrane Proteins**

Survival, hydroxyl radical formation, and membrane depolarization of wild-type *E. coli* (black squares),  $\Delta hflK\Delta cpxA$  (blue triangles),  $\Delta hflK\Delta arcA$  (brown triangles),  $\Delta secG\Delta cpxA$  (red circles), and  $\Delta secG\Delta arcA$  (green circles) after treatment with 5  $\mu$ g/ml gentamicin.

(A) Percent survival of each strain relative to when gentamicin treatment started (0 hr).

(B and C) Fluorescence for each strain relative to the maximum fluorescence achieved in the wild-type background using the hydroxyl radical detecting dye, HPF (B), or the membrane depolarization dye DIBAC<sub>4</sub>(3) (C).

knocked out in these strains (Figure 6). In all cases, the rate of killing, hydroxyl radical levels, and membrane depolarization among the double knockouts ( $\Delta secG\Delta cpxA$ ,  $\Delta secG\Delta arcA$ ,  $\Delta hflK\Delta cpxA$ , and  $\Delta hflK\Delta arcA$ ) were more similar to those in  $\Delta arcA$  and  $\Delta cpxA$  (Figures 4 and 5A) than to those in  $\Delta secG$  and  $\Delta hflK$  (Figures 3A and 4). These data show that the trafficking of mistranslated proteins into or across the inner membrane is a critical component of hydroxyl radical formation through activation of the Cpx and Arc two-component systems.

### DISCUSSION

In this study, we focused on aminoglycoside antibiotics and uncovered the specific trigger by which the aminoglycoside-ribosome

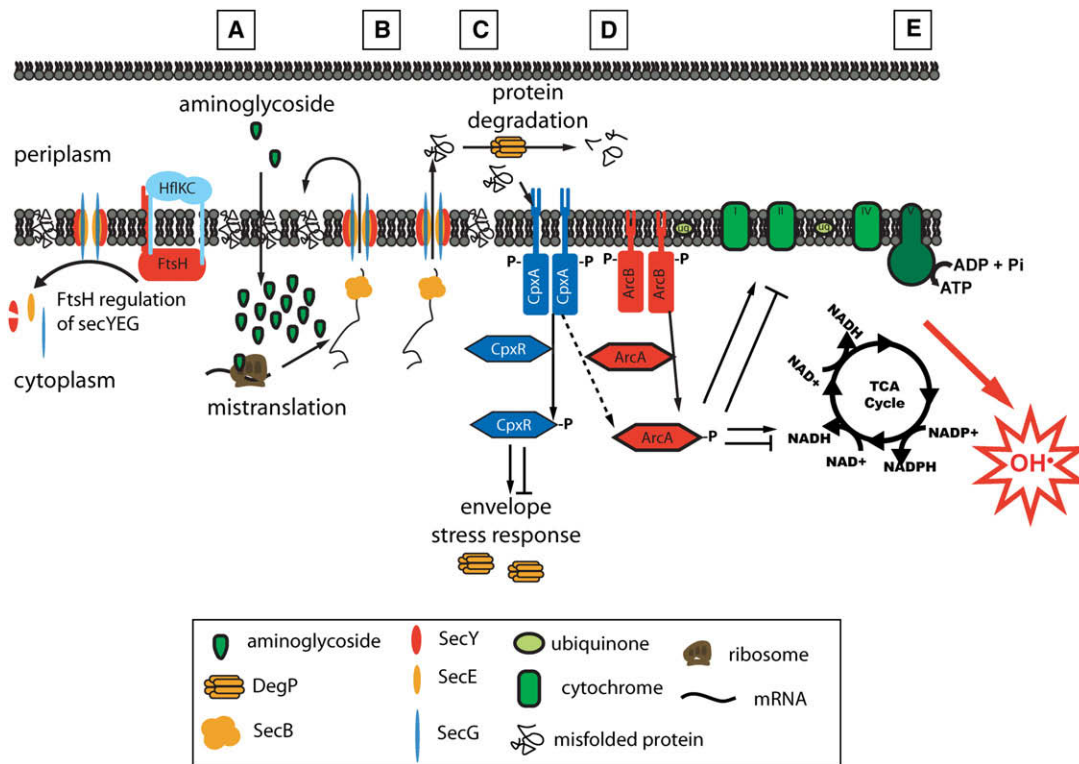


**Figure 7. Proposed Mechanism by which Aminoglycosides Trigger Hydroxyl Radical Formation and Cell Death**

The primary interaction between the aminoglycoside and ribosome causes protein mistranslation (A). Mistranslated, immature membrane proteins are brought to membrane translocation complexes (e.g., SecYEG) by chaperone proteins (SecB) and are translocated across the inner membrane into the periplasmic space or inserted into the membrane (B). Because of mistranslation, many of these proteins are misfolded, leading to phosphorylation of CpxA (C). Activated CpxA phosphorylates CpxR, which upregulates expression of envelope stress-response proteins, such as the periplasmic protease DegP (D). CpxA may also activate ArcA, which regulates a large number of metabolic and respiratory genes. These changes shift the cell into a state that provokes free radical formation, ultimately culminating in hydroxyl radical formation and cell death (E). We found that  $\beta$ -lactams and quinolones also trigger hydroxyl radical formation and cell death through the Cpx and Arc two-component systems (D and E); the specific triggers for  $\beta$ -lactams and quinolones remain to be worked out.

interaction stimulates the hydroxyl radical component of cell death. On the basis of our findings, we propose the following integrated model whereby aminoglycosides trigger hydroxyl radical formation (Figure 7). The primary result of the aminoglycoside-ribosome interaction is an increase in tRNA mismatching resulting in protein mistranslation (Figure 7A), a phenotype not seen with the bacteriostatic ribosome inhibitors in *E. coli*. Critically, in our proposed mechanism, some of these mistranslated proteins are brought to membrane translocation complexes (e.g., SecYEG) by chaperone proteins (SecB) and translocated across the inner membrane into the periplasmic space or inserted into the membrane (Figure 7B). As a consequence of aminoglycoside-induced mistranslation, some of these membrane-bound proteins are misfolded, which activates the envelope two-component stress-response sensor, CpxA (Figure 7C). Activated CpxA phosphorylates CpxR, which upregulates expression of envelope stress-response proteins, such as the periplasmic protease DegP, in order to protect the cell against the increase in misfolded proteins in the membrane and periplasm. CpxA may also activate the redox-responsive two-component transcription factor, ArcA (Iuchi et al., 1989; Ronson et al., 1987) (Figure 7D). Our results suggest that activation of the envelope

stress-response system, together with ArcA-regulated changes in metabolic and respiratory systems, pushes the cell into a state that provokes oxidative stress, ultimately resulting in hydroxyl radical formation and cell death (Figure 7E). The mechanism by which the initial activation of metabolic and respiratory systems occurs is unknown and requires further exploration.

Aminoglycosides bring about a number of physiological and biochemical changes associated with the lethal event. These include changes in membrane integrity, ribosome function, and oxidative stress (Hancock, 1981; Kohanski et al., 2007). Our work with the envelope stress-response knockouts (Figures 4 and 5) suggests that aminoglycosides employ multiple mechanisms to ensure efficient cellular death. The correlation between survival and membrane depolarization (Figures 4 and 5) points toward gradual changes in membrane integrity as a key component underlying the radical-independent mode of killing. This may be due to accumulation over time of damaged proteins in the membrane (Davis et al., 1986). As a whole, our work suggests that the role of radical formation after aminoglycoside treatment accounts for the observed initial, rapid decrease in cell viability.

We found that mistranslation of envelope proteins and subsequent activation of the envelope stress response is the specific

trigger for aminoglycoside-induced hydroxyl radical formation (Figures 7C–7E). Two-component systems are particularly useful in fast transitions between different environments (Hoch, 2000), and it is interesting that a fast, protective response to misfolded envelope proteins stimulated by CpxA activation also leads to hydroxyl radical formation (Figure 7). Intuitively, we would expect the observed upregulation in expression of the periplasmic protease *degP* (Figure 4E), to be a protective response against cell death related to mistranslation and accumulation of corrupt periplasmic proteins. However, removal of *degP* and the envelope stress-response two-component transcription factor, *cpxR*, led to a decrease in radical formation and a significant delay in the rate of killing after aminoglycoside treatment (Figures 5A and 5B). The Cpx system is controlled by a tight feedback loop that allows for fast switching between an on and off state (Raivio et al., 1999). This feedback mechanism involves the CpxR-regulated periplasmic protein CpxP (Danese and Silhavy, 1998a). CpxP, which is degraded by DegP, negatively regulates the activity of CpxA (Buelow and Raivio, 2005). It is possible that increased degradation of CpxP in the periplasmic space by DegP relieves CpxP-mediated repression of CpxA and enhances the rate of signaling via CpxA, ultimately leading to hydroxyl radical formation (Figures 7C–7E) through a mechanism that likely involves ArcA. Our data (Figure 5) also suggest that oxidative stress triggered by incorporation of mistranslated proteins in the cell envelope and the fast switching capabilities of the two-component systems are critical for the initial, rapid, radical-dependent killing after aminoglycoside treatment.

Importantly, our results point toward a broad role for the redox response and envelope stress-response two-component systems in bactericidal antibiotic-induced cell death (Figures 7D and 7E). It is likely that the role of ArcA here is through modulation of cellular metabolism, and additional efforts are required for determination of how ArcA, together with other regulatory elements including transcription factors and metabolite cofactors, affects metabolism after antibiotic exposure. ArcA-mediated changes in metabolism and respiration are also likely to be important in the common oxidative damage cell death pathway after exposure to bactericidal antibiotics (Kohanski et al., 2007). The involvement of the Cpx system in antibiotic-mediated cell death shows that membrane integrity is crucial for bacterial survival. In the case of  $\beta$ -lactams, membrane integrity is affected directly by the drug-target interaction, whereas with aminoglycosides, membrane function and integrity appears to be most affected by drug-induced protein mistranslation. The relationship between quinolone antibiotics and the membrane is less clear. Treatment with the DNA gyrase inhibitor nalidixic acid has been associated with changes in the protein to lipid ratio in the cell envelope (Dougherty and Saukkonen, 1985). Quinolones do induce filamentation, and it is possible that changes in membrane composition, function, and integrity brought about by an increase in cell size affect Cpx signaling and cell death.

Aminoglycoside-induced mistranslation in *E. coli* is specifically due to the interaction of the drug with the ribosome (Figure 7A). Variability in the structure of the ribosome may affect the induction of mistranslation by aminoglycosides and may also induce mistranslation by other classes of ribosome inhibitors. Interestingly, ribosomal RNA sequences vary among bacterial

species, and some ribosome inhibitors are bacteriostatic in certain species and bactericidal in others. For example, chloramphenicol is bacteriostatic against *E. coli* but bactericidal against *Haemophilus influenza* (Rahal and Simberkoff, 1979). It is possible that the variability in ribosomal RNA sequences causes some ribosome inhibitors to induce mistranslation and subsequent misfolding of membrane proteins, thereby lowering the threshold for hydroxyl radical formation and cell death in certain bacterial species, whereas in other species these same ribosome inhibitors do not induce mistranslation and are merely bacteriostatic. A deeper understanding of this lethal trigger may allow us to convert bacteriostatic ribosome inhibitors into bactericidal drugs by identifying targets that induce protein mistranslation and thereby trigger radical-based cell death.

The membrane regulatory proteins HflKC and SecG (Figure 7B), knockouts of which we have shown enhance aminoglycoside lethality, interact with essential proteins (FtsH and SecE/SecY, respectively) but are not essential themselves (Economou, 1999; Gottesman, 1996). Additionally, SecG is not conserved outside of bacteria, whereas SecE and SecY are well conserved in humans (Economou, 1999). Earlier work on glycolipid derivatives of vancomycin (Eggert et al., 2001) has shown that targeting nonessential genes is a viable option for enhancing antibiotic efficacy. As combination therapy approaches are explored further (Cottarel and Wierzbowski, 2007), it is possible that nonessential regulators of essential proteins will turn out to be high-quality drug targets for potentiation of known antibacterial drugs.

Aminoglycosides are a powerful, broad-spectrum class of antibiotics with excellent activity against common infections involving Gram-negative bacteria. However, this class of drugs has a limited therapeutic index due to nephrotoxicity (Mingeot-Leclercq and Tulkens, 1999) and ototoxicity (Wu et al., 2002) at higher dosages (e.g., peak serum concentration greater than 12–15  $\mu\text{g/ml}$  for gentamicin [Zaske et al., 1982]). Because of the increasing prevalence of resistant bacteria, the effectiveness of this drug class may become limited. Targeting of HflKC or SecG as part of a combination therapy could enhance the potency of aminoglycosides, broadening their therapeutic index at lower, nontoxic dosages and possibly sensitizing clinically resistant strains.

## EXPERIMENTAL PROCEDURES

### Media and Antibiotics

All experiments were performed in Luria-Bertani (LB) medium (Fisher Scientific, Pittsburgh, PA). For all experiments, we used the aminocyclitol family antibiotics kanamycin (Fisher Scientific), gentamicin (Sigma, St. Louis, MO), or spectinomycin (MP Biomedicals).

### Strains

Screening for aminoglycoside sensitivity was performed in the *E. coli* single-gene knockout library (BW25113 background) (Baba et al., 2006) (Table S7). All other experiments were performed with MG1655- (ATCC 700926) (Table S7) derived strains. All single and double knockouts were constructed through the use of P1 phage transduction, and P1 stock was derived from the *E. coli* knockout library (Baba et al., 2006) (Table S7). Positive P1 transductants were confirmed by acquisition of kanamycin resistance and PCR. Removal of the kanamycin-resistance cassette was accomplished with the *pcp20*

plasmid (Datsenko and Wanner, 2000) (Table S7) and confirmed by PCR prior to experimentation.

### Screen of *E. coli* Knockout Library for Growth Changes in the Presence of Gentamicin

To identify single-gene deletions in *E. coli* that enhanced aminoglycoside activity, we initially screened a single-deletion *E. coli* knockout library (Baba et al., 2006) with gentamicin. For this study, the library was converted from 96- to 384-well format (Table S3). Each 384-well plate of this kanamycin-resistant library was grown in LB media containing 25 µg/ml kanamycin (75 µl/well) to stationary phase at 37°C without shaking. The overnight cultures were diluted (1:375) with a 384 pin replicator (0.2 µl/pin) into 384-well treatment plates containing LB media plus 5 µg/ml gentamicin (75 µl/well) or control plates containing LB media only (75 µl/well). These plates were incubated for 24 hr at 37°C without shaking. We note that shaking is known to enhance aminoglycoside uptake by keeping cultures well aerated (Taber et al., 1987); however, the purpose of these experiments was to isolate candidate genes for further detailed analysis. Additionally, shaking was not employed with the 384-well plates so that cross-contamination between individual wells could be avoided and because it is difficult to generate sufficient turbulence within a 75 µl volume to aerate the cultures. So that propagation of false leads from this dataset could be limited, all additional experiments of individual strains were done in well-aerated flasks with shaking. Optical density at 600 nm (OD600) for all plates was determined (Table S3) with a SPECTRAFluor Plus (Tecan).

After removing knockouts that exhibited no growth when untreated, we examined the distribution of the ratio of treated OD600 to control (untreated) OD600 and considered the upper and lower 5% of ratios as growth outliers (Table S3). There were 11 knockouts exhibiting decreased growth in the presence of gentamicin, and 303 knockouts showing increased growth in the presence of gentamicin (Table S3).

### Growth Conditions

In our experiments, we compared the survival of gentamicin-treated wild-type exponential phase *E. coli* to the survival of the various deletion strains (Table S7) treated with gentamicin. In brief, cultures were grown in 25 ml LB in 250 ml flasks and incubated at 37°C and 300 RPM; gentamicin was added at early exponential phase at a concentration of 5 µg/ml. This protocol was also used for experiments with norfloxacin (250 ng/ml, 100 ng/ml), ampicillin (5 µg/ml, 3 µg/ml), kanamycin (5 µg/ml), spectinomycin (400 µg/ml), and a higher concentration of gentamicin (15 µg/ml). Colony-forming units per ml were determined as previously described (Kohanski et al., 2007). All experiments were performed in light-insulated shakers to ensure that light-induced redox cycling of antibiotics (Martin et al., 1987; Umezawa et al., 1997) was not a confounding factor.

### Hydroxyl Radical and Membrane Potential Experiments Using the Flow Cytometer

To detect hydroxyl radical formation, we used the fluorescent reporter dye 3'-(p-hydroxyphenyl) fluorescein (HPF, Invitrogen, Carlsbad, CA). Samples were collected at 1 hr intervals after addition of gentamicin and resuspended in 500 µl of 1 × PBS (pH 7.2) (Fisher Scientific) containing 10 µM HPF. Samples were incubated in the dark for 15 min; the cells were then pelleted, the supernatant removed, and the cells resuspended in 1 ml sterile filtered 1 × PBS for fluorescence-activated cell sorting (FACS) analysis. The following photomultiplier tube (PMT) voltage settings were used: E00 (FSC), 360 (SSC), and 825 (FL1). To monitor changes in membrane potential, we used the fluorescent reporter dye bis-(1,3-dibutylbarbituric acid) trimethine oxonol [DiBAC<sub>4</sub>(3), Invitrogen]. Samples were collected at 1 hr intervals after addition of gentamicin and resuspended in 1 ml of 1 × PBS containing 10 µg/ml DiBAC<sub>4</sub>(3). Samples were incubated in the dark for 15 min and then analyzed on the FACS. The following PMT voltage settings were used: E00 (FSC), 360 (SSC), and 550 (FL1). All data were collected with a Becton Dickinson FACSCalibur flow cytometer (Becton Dickinson, San Jose, CA) with a 488 nm argon laser and a 515 to 545 nm emission filter (FL1) at low flow rate. At least 150,000 cells were collected for each sample. Calibrite beads (Becton Dickinson) were used for instrument calibration. Flow data were processed and analyzed with MATLAB (MathWorks, Natick, MA).

### Gene Expression Analysis

We compared the microarray-determined mRNA profiles (Affymetrix *E. coli* Antisense2 genome arrays) of wild-type *E. coli* cultures treated with an aminoglycoside (5 µg/ml gentamicin) to those treated with a bacteriostatic ribosome inhibitor (400 µg/ml spectinomycin). Gene expression profiles can be found at <http://m3d.bu.edu/>. For all experiments, overnight cultures were diluted 1:500 into 250 ml LB in 1 liter flasks for collection of total RNA. Early exponential phase cultures were split (50 ml LB into 3 × 250 ml flasks) and antibiotics added as described above. Untreated control samples were also collected. Samples for microarray analysis were taken immediately before treatment (time zero) and then at 30, 60, and 120 min after treatment. RNA collection and microarray processing were done as previously described (Kohanski et al., 2007). In addition, we compared the microarray-determined (Affymetrix *E. coli* Antisense2 genome arrays) mRNA profiles from a previously collected time course (Kohanski et al., 2007) of wild-type *E. coli* cultures treated with a bactericidal antibiotic (5 µg/ml kanamycin) to those treated with a bacteriostatic antibiotic (400 µg/ml spectinomycin).

The resulting microarray \*.CEL files from the gentamicin time course described above were combined with \*.CEL files from microarrays that comprise the M3D compendium (Faith et al., 2007) (<http://m3d.bu.edu/>; E\_coli\_v3\_Build\_3) and RMA normalized (Bolstad et al., 2003) with RMAexpress, for a total of 534 RMA-normalized *E. coli* expression microarrays. These were analyzed as previously described (Kohanski et al., 2007). In brief, each gene's standard deviation of expression,  $\sigma$ , was calculated and used for construction of the z scale difference between that gene's normalized expression in gentamicin or kanamycin treatment (bactericidal aminoglycoside drug treatment) versus a spectinomycin treatment (bacteriostatic drug treatment):

$$\Delta z_{\text{exp}} = \frac{X_{\text{exp}} - X_{\text{ctrl}}}{\sigma}$$

This allowed us to measure each gene's change in expression for a given experiment in units of standard deviation, a form of the z test. For each time point in the experiment set, we converted  $\Delta z$  scores to p values and chose significantly up- and downregulated genes by selecting those with a q value less than 0.05 (false discovery rate) (Storey and Tibshirani, 2003). We merged the resultant gene lists across all time points (set union) to obtain a coarse profile of the difference in expression between gentamicin and spectinomycin, as well as the differences between kanamycin and spectinomycin (Table S1).

### Gene Network Analysis

Gene networks were isolated from the  $\Delta z$ -based list of up- and downregulated genes. We used the CLR map (Faith et al., 2007) created from the M3D compendium (E\_coli\_v3\_Build\_3) to generate the set of all possible connections between genes, using a CLR threshold of 60% precision as the cutoff for a true connection (Faith et al., 2007). From this set of all possible gene connections, we kept all direct connections between genes whose expression changed significantly, as well as connections where significantly changing genes are separated by one nonperturbed intermediate gene. All remaining connections between perturbed and nonperturbed genes were removed. This allowed us to group significantly changing genes (Table S3) on the basis of a functional connectivity map (CLR).

For additional pathway-level insights, we performed Gene Ontology-based enrichment (Ashburner et al., 2000; Camon et al., 2004) on the gene networks using GO::TermFinder (Boyle et al., 2004), requiring pathway enrichment q values to be less than 0.05 and setting the p value estimation mode to bootstrapping. Transcription factor enrichment was performed as previously described (Dwyer et al., 2007) with RegulonDB (Salgado et al., 2006) and CLR (Faith et al., 2007) predictions (cutoff of 60% precision) used as the set of possible transcription factor interactions.

### RNA Extraction, Reverse Transcription, and qPCR Analysis

For qPCR analysis, RNA was extracted from the control strain MG1655, as well as  $\Delta arcA$ ,  $\Delta arcB$ ,  $\Delta cpxA$  and  $\Delta cpxR$ , after treatment with 5 µg/ml gentamicin under the growth conditions described above. Samples were collected at 0, 30, 60, and 120 min after gentamicin addition for three biological replicates of each strain. Samples were collected at volumes of 0.5 ml culture volume

per 0.3 OD<sub>600</sub>, stabilized immediately with 2× volume of RNAprotect Bacterial Reagent (QIAGEN) as per the manufacturer's instructions, and stored overnight at −80°C. Total RNA was extracted with QIAGEN RNeasy Mini spin columns according to the manufacturer's instructions. Total RNA was treated with RNase-free DNase (Ambion, Austin, TX). For each sample, reverse transcription of 2 μg total RNA was performed with the Superscript III Reverse Transcriptase kit (Invitrogen) in a total volume of 20 μl according to the manufacturer's instructions.

qPCR primers for each transcript of interest (Table S8) and the reference transcripts *rnsA* and *rnsB* were designed with sequences found in the EcoCyc database (Karp et al., 2007) and PrimerQuest software (IDT, <http://www.idtdna.com/>). For all primer pairs, amplicon size was ~100 bp, the calculated primer annealing temperature was 60°C, and probabilities of primer-dimer/hairpin formations were minimized. Primer specificity was confirmed with gel electrophoresis. qPCR reactions using DyNAmo HS SYBR Green qPCR Kit (Finnzymes) were prepared according to manufacturer's instructions with 2 μl of a 1:10 dilution of cDNA (~20 ng of total RNA) in a total volume of 20 μl containing 300 nM of forward primers and 300 nM of reverse primers, 10 μl 2× SYBR Green Master Mix, and 0.1 μl ROX passive reference dye. Reactions were carried out in 384-well optical microplates (Applied Biosystems) with an ABI Prism 7900 HT. Crossing-point threshold (Ct) and real-time fluorescence data were obtained with the ABI Prism Sequence Detection Software v2.0 with default software parameters. Expression levels were obtained from Ct values as previously described (Gardner et al., 2003).

## SUPPLEMENTAL DATA

Supplemental Data include Supplemental Results and Discussion, Supplemental Experimental Procedures, 11 figures, and eight tables and can be found with this article online at [http://www.cell.com/supplemental/S0092-8674\(08\)01195-1](http://www.cell.com/supplemental/S0092-8674(08)01195-1).

## ACKNOWLEDGMENTS

We thank N. Gerry for processing the microarrays and B. Hayete for helpful discussions on gene expression analysis. We thank M. DePristo for comments on the manuscript. This work was supported by the National Institutes of Health (NIH) through the NIH Director's Pioneer Award Program, grant number DP1 OD003644, the National Science Foundation (NSF) Frontiers in Integrative Biological Research program, NSF award EMSW21-RTG, and the Howard Hughes Medical Institute.

Received: November 13, 2007

Revised: July 14, 2008

Accepted: September 15, 2008

Published: November 13, 2008

## REFERENCES

- Akiyama, Y., Kihara, A., Tokuda, H., and Ito, K. (1996). FtsH (HflB) is an ATP-dependent protease selectively acting on SecY and some other membrane proteins. *J. Biol. Chem.* 271, 31196–31201.
- Ashburner, M., Ball, C.A., Blake, J.A., Botstein, D., Butler, H., Cherry, J.M., Davis, A.P., Dolinski, K., Dwight, S.S., Eppig, J.T., et al. (2000). Gene ontology: Tool for the unification of biology. The Gene Ontology Consortium. *Nat. Genet.* 25, 25–29.
- Baba, T., Ara, T., Hasegawa, M., Takai, Y., Okumura, Y., Baba, M., Datsenko, K.A., Tomita, M., Wanner, B.L., and Mori, H. (2006). Construction of *Escherichia coli* K-12 in-frame, single-gene knockout mutants: The Keio collection. *Mol. Syst. Biol.* 2, 2006.0008.
- Bolstad, B.M., Irizarry, R.A., Astrand, M., and Speed, T.P. (2003). A comparison of normalization methods for high density oligonucleotide array data based on variance and bias. *Bioinformatics* 19, 185–193.
- Boyle, E.I., Weng, S., Gollub, J., Jin, H., Botstein, D., Cherry, J.M., and Sherlock, G. (2004). GO:TermFinder—open source software for accessing Gene Ontology information and finding significantly enriched Gene Ontology terms associated with a list of genes. *Bioinformatics* 20, 3710–3715.
- Bryan, L.E., and Kwan, S. (1983). Roles of ribosomal binding, membrane potential, and electron transport in bacterial uptake of streptomycin and gentamicin. *Antimicrob. Agents Chemother.* 23, 835–845.
- Buelow, D.R., and Raivio, T.L. (2005). Cpx signal transduction is influenced by a conserved N-terminal domain in the novel inhibitor CpxP and the periplasmic protease DegP. *J. Bacteriol.* 187, 6622–6630.
- Camon, E., Magrane, M., Barrell, D., Lee, V., Dimmer, E., Maslen, J., Binns, D., Harte, N., Lopez, R., and Apweiler, R. (2004). The Gene Ontology Annotation (GOA) Database: Sharing knowledge in Uniprot with Gene Ontology. *Nucleic Acids Res.* 32, D262–D266.
- Cottarel, G., and Wierzbowski, J. (2007). Combination drugs, an emerging option for antibacterial therapy. *Trends Biotechnol.* 25, 547–555.
- Danese, P.N., and Silhavy, T.J. (1998a). CpxP, a stress-combative member of the Cpx regulon. *J. Bacteriol.* 180, 831–839.
- Danese, P.N., and Silhavy, T.J. (1998b). Targeting and assembly of periplasmic and outer-membrane proteins in *Escherichia coli*. *Annu. Rev. Genet.* 32, 59–94.
- Danese, P.N., Snyder, W.B., Cosma, C.L., Davis, L.J., and Silhavy, T.J. (1995). The Cpx two-component signal transduction pathway of *Escherichia coli* regulates transcription of the gene specifying the stress-inducible periplasmic protease, DegP. *Genes Dev.* 9, 387–398.
- Datsenko, K.A., and Wanner, B.L. (2000). One-step inactivation of chromosomal genes in *Escherichia coli* K-12 using PCR products. *Proc. Natl. Acad. Sci. USA* 97, 6640–6645.
- Davis, B.D. (1987). Mechanism of bactericidal action of aminoglycosides. *Microbiol. Rev.* 51, 341–350.
- Davis, B.D., Chen, L.L., and Tai, P.C. (1986). Misread protein creates membrane channels: An essential step in the bactericidal action of aminoglycosides. *Proc. Natl. Acad. Sci. USA* 83, 6164–6168.
- Dougherty, T.J., and Saukkonen, J.J. (1985). Membrane permeability changes associated with DNA gyrase inhibitors in *Escherichia coli*. *Antimicrob. Agents Chemother.* 28, 200–206.
- Duguay, A.R., and Silhavy, T.J. (2004). Quality control in the bacterial periplasm. *Biochim. Biophys. Acta* 1694, 121–134.
- Dukan, S., Farewell, A., Ballesteros, M., Taddei, F., Radman, M., and Nystrom, T. (2000). Protein oxidation in response to increased transcriptional or translational errors. *Proc. Natl. Acad. Sci. USA* 97, 5746–5749.
- Dwyer, D.J., Kohanski, M.A., Hayete, B., and Collins, J.J. (2007). Gyrase inhibitors induce an oxidative damage cellular death pathway in *Escherichia coli*. *Mol. Syst. Biol.* 3, 91.
- Economou, A. (1999). Following the leader: Bacterial protein export through the Sec pathway. *Trends Microbiol.* 7, 315–320.
- Eggert, U.S., Ruiz, N., Falcone, B.V., Branstrom, A.A., Goldman, R.C., Silhavy, T.J., and Kahne, D. (2001). Genetic basis for activity differences between vancomycin and glycolipid derivatives of vancomycin. *Science* 294, 361–364.
- Faith, J.J., Hayete, B., Thaden, J.T., Mogno, I., Wierzbowski, J., Cottarel, G., Kasif, S., Collins, J.J., and Gardner, T.S. (2007). Large-scale mapping and validation of *Escherichia coli* transcriptional regulation from a compendium of expression profiles. *PLoS Biol.* 5, e8.
- Gardner, T.S., di Bernardo, D., Lorenz, D., and Collins, J.J. (2003). Inferring genetic networks and identifying compound mode of action via expression profiling. *Science* 301, 102–105.
- Georgellis, D., Kwon, O., and Lin, E.C. (2001). Quinones as the redox signal for the arc two-component system of bacteria. *Science* 292, 2314–2316.
- Gottesman, S. (1996). Proteases and their targets in *Escherichia coli*. *Annu. Rev. Genet.* 30, 465–506.
- Hancock, R.E. (1981). Aminoglycoside uptake and mode of action with special reference to streptomycin and gentamicin. II. Effects of aminoglycosides on cells. *J. Antimicrob. Chemother.* 8, 429–445.

- Hartl, F.U., Lecker, S., Schiebel, E., Hendrick, J.P., and Wickner, W. (1990). The binding cascade of SecB to SecA to SecY/E mediates preprotein targeting to the *E. coli* plasma membrane. *Cell* **63**, 269–279.
- Hoch, J.A. (2000). Two-component and phosphorelay signal transduction. *Curr. Opin. Microbiol.* **3**, 165–170.
- Iuchi, S., Furlong, D., and Lin, E.C. (1989). Differentiation of *arcA*, *arcB*, and *cpxA* mutant phenotypes of *Escherichia coli* by sex pilus formation and enzyme regulation. *J. Bacteriol.* **171**, 2889–2893.
- Jepras, R.I., Paul, F.E., Pearson, S.C., and Wilkinson, M.J. (1997). Rapid assessment of antibiotic effects on *Escherichia coli* by bis-(1,3-dibutylbarbituric acid) trimethine oxonol and flow cytometry. *Antimicrob. Agents Chemother.* **41**, 2001–2005.
- Karp, P.D., Keseler, I.M., Shearer, A., Latendresse, M., Krummenacker, M., Paley, S.M., Paulsen, I., Collado-Vides, J., Gama-Castro, S., Peralta-Gil, M., et al. (2007). Multidimensional annotation of the *Escherichia coli* K-12 genome. *Nucleic Acids Res.* **35**, 7577–7590.
- Kihara, A., Akiyama, Y., and Ito, K. (1996). A protease complex in the *Escherichia coli* plasma membrane: HflKC (HflA) forms a complex with FtsH (HflB), regulating its proteolytic activity against SecY. *EMBO J.* **15**, 6122–6131.
- Kihara, A., Akiyama, Y., and Ito, K. (1997). Host regulation of lysogenic decision in bacteriophage lambda: Transmembrane modulation of FtsH (HflB), the cII degrading protease, by HflKC (HflA). *Proc. Natl. Acad. Sci. USA* **94**, 5544–5549.
- Kihara, A., Akiyama, Y., and Ito, K. (1999). Dislocation of membrane proteins in FtsH-mediated proteolysis. *EMBO J.* **18**, 2970–2981.
- Kohanski, M.A., Dwyer, D.J., Hayete, B., Lawrence, C.A., and Collins, J.J. (2007). A common mechanism of cellular death induced by bactericidal antibiotics. *Cell* **130**, 797–810.
- Liu, X., and De Wulf, P. (2004). Probing the ArcA-P modulon of *Escherichia coli* by whole genome transcriptional analysis and sequence recognition profiling. *J. Biol. Chem.* **279**, 12588–12597.
- Luirink, J., and Sinning, I. (2004). SRP-mediated protein targeting: Structure and function revisited. *Biochim. Biophys. Acta* **1694**, 17–35.
- Malpica, R., Franco, B., Rodriguez, C., Kwon, O., and Georgellis, D. (2004). Identification of a quinone-sensitive redox switch in the ArcB sensor kinase. *Proc. Natl. Acad. Sci. USA* **101**, 13318–13323.
- Martin, J.P., Jr., Colina, K., and Logsdon, N. (1987). Role of oxygen radicals in the phototoxicity of tetracyclines toward *Escherichia coli* B. *J. Bacteriol.* **169**, 2516–2522.
- Matsumoto, G., Mori, H., and Ito, K. (1998). Roles of SecG in ATP- and SecA-dependent protein translocation. *Proc. Natl. Acad. Sci. USA* **95**, 13567–13572.
- Mingeot-Leclercq, M.P., and Tulkens, P.M. (1999). Aminoglycosides: Nephrotoxicity. *Antimicrob. Agents Chemother.* **43**, 1003–1012.
- Mori, H., and Ito, K. (2001). The Sec protein-translocation pathway. *Trends Microbiol.* **9**, 494–500.
- Pogliano, J., Lynch, A.S., Belin, D., Lin, E.C., and Beckwith, J. (1997). Regulation of *Escherichia coli* cell envelope proteins involved in protein folding and degradation by the Cpx two-component system. *Genes Dev.* **11**, 1169–1182.
- Rahal, J.J., Jr., and Simberkoff, M.S. (1979). Bactericidal and bacteriostatic action of chloramphenicol against meningial pathogens. *Antimicrob. Agents Chemother.* **16**, 13–18.
- Raivio, T.L., Popkin, D.L., and Silhavy, T.J. (1999). The Cpx envelope stress response is controlled by amplification and feedback inhibition. *J. Bacteriol.* **181**, 5263–5272.
- Ronson, C.W., Nixon, B.T., and Ausubel, F.M. (1987). Conserved domains in bacterial regulatory proteins that respond to environmental stimuli. *Cell* **49**, 579–581.
- Ruiz, N., and Silhavy, T.J. (2005). Sensing external stress: Watchdogs of the *Escherichia coli* cell envelope. *Curr. Opin. Microbiol.* **8**, 122–126.
- Saikawa, N., Akiyama, Y., and Ito, K. (2004). FtsH exists as an exceptionally large complex containing HflKC in the plasma membrane of *Escherichia coli*. *J. Struct. Biol.* **146**, 123–129.
- Salgado, H., Gama-Castro, S., Peralta-Gil, M., Diaz-Peredo, E., Sanchez-Solano, F., Santos-Zavaleta, A., Martinez-Flores, I., Jimenez-Jacinto, V., Bonavides-Martinez, C., Segura-Salazar, J., et al. (2006). RegulonDB (version 5.0): *Escherichia coli* K-12 transcriptional regulatory network, operon organization, and growth conditions. *Nucleic Acids Res.* **34**, D394–D397.
- Setsukinai, K., Urano, Y., Kakinuma, K., Majima, H.J., and Nagano, T. (2003). Development of novel fluorescence probes that can reliably detect reactive oxygen species and distinguish specific species. *J. Biol. Chem.* **278**, 3170–3175.
- Storey, J.D., and Tibshirani, R. (2003). Statistical significance for genomewide studies. *Proc. Natl. Acad. Sci. USA* **100**, 9440–9445.
- Strauch, K.L., Johnson, K., and Beckwith, J. (1989). Characterization of degP, a gene required for proteolysis in the cell envelope and essential for growth of *Escherichia coli* at high temperature. *J. Bacteriol.* **171**, 2689–2696.
- Taber, H.W., Mueller, J.P., Miller, P.F., and Arrow, A.S. (1987). Bacterial uptake of aminoglycoside antibiotics. *Microbiol. Rev.* **51**, 439–457.
- Umezawa, N., Arakane, K., Ryu, A., Mashiko, S., Hirobe, M., and Nagano, T. (1997). Participation of reactive oxygen species in phototoxicity induced by quinolone antibacterial agents. *Arch. Biochem. Biophys.* **342**, 275–281.
- Vakulenko, S.B., and Mobashery, S. (2003). Versatility of aminoglycosides and prospects for their future. *Clin. Microbiol. Rev.* **16**, 430–450.
- Weisblum, B., and Davies, J. (1968). Antibiotic inhibitors of the bacterial ribosome. *Bacteriol. Rev.* **32**, 493–528.
- Wickner, W., and Schekman, R. (2005). Protein translocation across biological membranes. *Science* **310**, 1452–1456.
- Wu, W.J., Sha, S.H., and Schacht, J. (2002). Recent advances in understanding aminoglycoside ototoxicity and its prevention. *Audiol. Neurootol.* **7**, 171–174.
- Zaske, D.E., Cipolle, R.J., Rotschafer, J.C., Solem, L.D., Mosier, N.R., and Strate, R.G. (1982). Gentamicin pharmacokinetics in 1,640 patients: Method for control of serum concentrations. *Antimicrob. Agents Chemother.* **21**, 407–411.